

Solvation of cyclopentadienyl and substituted cyclopentadienyl radicals in small clusters. II. Cyanocyclopentadienyl with polar solvents

J. Yao, J. A. Fernandez, and E. R. Bernstein

Citation: *The Journal of Chemical Physics* **110**, 5174 (1999); doi: 10.1063/1.478412

View online: <http://dx.doi.org/10.1063/1.478412>

View Table of Contents: <http://aip.scitation.org/toc/jcp/110/11>

Published by the *American Institute of Physics*

COMPLETELY

REDESIGNED!



**PHYSICS
TODAY**

Physics Today Buyer's Guide
Search with a purpose.

Solvation of cyclopentadienyl and substituted cyclopentadienyl radicals in small clusters. II. Cyanocyclopentadienyl with polar solvents

J. Yao, J. A. Fernandez, and E. R. Bernstein

Department of Chemistry, Colorado State University, Fort Collins, Colorado 80523-1872

(Received 11 March 1998; accepted 4 December 1998)

Clusters of the cyanocyclopentadienyl (CNcpd) radical and several polar solvent molecules (e.g., CF_2H_2 , CF_3H , CF_3Cl , CH_3Cl , ROH , H_2O) created in a supersonic jet expansion are studied by laser induced fluorescence and hole burning spectroscopies. Lennard-Jones–Coulomb atom–atom potential energy calculations are employed in combination with *ab initio* calculations to aid in the interpretation of the observed spectra and to understand the nature of the radical polar solvent solvation behavior. The calculations predict quite reasonable cluster binding energies and structures, but are less accurate in predicting van der Waals vibrational mode energies and cluster spectroscopic shifts. The limitations of the atom–atom potential energy surface model in dealing with the more subtle aspects of CNcpd–polar solvent intermolecular interactions are discussed. Some possible causes of inadequacies of the approach are presented. © 1999 American Institute of Physics. [S0021-9606(99)01310-0]

I. INTRODUCTION

Solvation studies for closed shell, stable molecules based on clusters formed in a supersonic expansion have been quite successful for both small and large molecular species.¹ Much less attention has been given to solvation studies involving open shell reactive intermediates, such as radicals. These latter systems are important for both condensed phase and gas phase chemistry and their behavior with regard to solvation is essential to their stability and reactivity. Radical open shell systems tend to be highly reactive and short lived and thus their solvation behavior is more difficult to study both experimentally and theoretically. Success in obtaining and interpreting spectra, and analyzing van der Waals (vdW) interactions and modes for open shell reactive intermediates in clusters has been achieved in only a limited number of instances. These solvation studies include OH ,² NH ,³ CH ,⁴ CN ,⁵ HCO ,⁶ $\text{C}_2\text{H}_3\text{O}$,⁷ CH_3O ,⁸ NCO ,⁹ $\text{C}_6\text{H}_5\text{CH}_2$,¹⁰ C_5H_5 ,¹¹ $\text{C}_5\text{H}_4\text{CH}_3$,¹¹ and a few others. Such radical solvation studies in the past have been mostly limited to nonpolar solvents. One expects that the behavior of radical–polar solvent clusters would be complex due to the increased solute–solvent interaction strength and the increased reactivity of species in the cluster.

In the preceding paper (paper I of this series of three reports), clusters of substituted cyclopentadienyl (Xcpd, $\text{X}=\text{H}$, F , CH_3 , CN) radicals with nonpolar solvents (Ar , N_2 , CH_4 , CF_4 , C_2F_6) are discussed. Cluster spectra for these systems are collected by fluorescence excitation (FE) and hole burning techniques. Extensive *ab initio* calculations^{12,13} coupled with empirical potential energy surface calculations are successfully employed to model the vdW interactions in these systems as they are evidenced by cluster structure, binding energies, vdW modes, and cluster spectroscopic shifts. The potential energy function of the Lennard-Jones–Coulomb form¹² requires a different set of parameters for each electronic state: these include atomic vdW radii (r_i),

atomic polarizabilities (α_i) and atomic partial charges (q_i) for each atom in the molecule comprising the cluster of interest. For ground state clusters, α_i and r_i are found by empirical data fitting and q_i can be determined accurately from *ab initio* algorithms.¹³ The values of α_i and r_i are derived by fitting an overwhelming amount of crystallographic and thermodynamic data and many types of atomic parameters appropriate for different chemical environments are determined.

Excited states can be treated in a similar manner but the fitting of α_i and r_i and the calculation of q_i are much less reliable because the data set is so small and the calculations are more complex. To model the excited state behavior of Xcpd–nonpolar solvent clusters we employ the Xcpd–Ar cluster data to fit C, H, X parameters under a number of simplifying assumptions.^{8,9,12} These parameters are in turn employed to understand the other cluster spectra; in general, this program is reasonably successful.

In this report, the spectra of vdW clusters of CNcpd and polar solvents (e.g., CH_2F_2 , CHF_3 , CF_3Cl , CH_3Cl , CH_3OH , H_2O) are discussed and interpreted based on the above algorithm. The same calculational procedures and radical parameters as described above are employed to explore the interactions for these new clusters. The calculations predict consistent geometries for clusters in their ground and excited states, suggesting that the ground and excited state potential energy surfaces are at least qualitatively correct. The predicted cluster binding energies, however, are not as accurate as are those found for nonpolar solvents because cluster spectral shifts are not well determined; in fact, the shifts are systematically predicted to be red and are actually found to be blue shifts. Rather than fit new parameters for the Lennard-Jones–Coulomb potential presented in paper I (preceding paper) to generate an acceptable fit to the polar cluster, we have chosen to use the previous parameters, potential format, and algorithm. This procedure highlights the essen-

tial differences between polar solvent and nonpolar solvent solvation for the CNcpd radical and allows one to explore and understand the behavior of the two general solvent classes. A number of possible causes for this systematic discrepancy are discussed, including missing terms in the potential energy function, poor parameters for the existing potential function, and the importance of hydrogen bonding in these systems.

II. PROCEDURES

A. Experimental

Laser induced fluorescence or fluorescence excitation experiments are described in paper I of this series and only a brief description of some of the particular details associated with the present systems are presented herein. The precursors used to generate CNcpd radicals are phenylazide ($C_6H_5N_3$, synthesized¹⁴) and phenyl isocyanate (C_6H_5NCO , Aldrich). A general valve pulsed nozzle is employed to generate the supersonic expansion into a stainless steel vacuum chamber. The expansion gas is He at ~ 100 – 200 psig. A 1 mm i.d. $\times 10$ mm long quartz tube is attached to the nozzle front flange. The radicals are generated inside the quartz tube by ArF excimer laser (193 nm, 80–100 mJ/pulse output) photolysis of the precursors. The solvent is mixed with the expansion gas and clusters form as the mixture cools in the adiabatic expansion from the quartz tube into the vacuum chamber.

A Nd/YAG pumped dye laser is used as the laser excitation source for the radicals and their clusters. The output of F548 dye in methanol is mixed with the Nd/YAG laser fundamental to achieve the appropriate wavelength range for CNcpd and CNcpd–solvent clusters. This laser beam intersects the molecular beam at about 15 mm downstream from the quartz tube exit. Fluorescence is collected by a 5 cm focal length lens and is focused on a C31034A RCA photomultiplier tube in a direction perpendicular to the coplanar laser and molecular beams. A UV330 filter attenuates scattered light from the excimer laser and other sources. For hole burning studies a second Nd/YAG pumped dye laser with the same output is set up to intersect the molecular beam 1 to 2 mm upstream from the first dye laser. This second laser is of higher output intensity and is set to trigger 0.5–1.0 μ s prior to the first laser. The first laser remains at a fixed frequency, while the second laser, firing earlier than the first, is scanned through the cluster spectrum.

B. Theory

The physical properties of CNcpd–polar solvent clusters are analyzed in this study as described in paper I of this series. For convenience we present the potential energy form (atom–atom, Lennard-Jones–Coulomb function) so that the later discussion and tables are more clear. The potential energy function is given by¹²

$$E = \sum_{i=1}^D \sum_{j=1}^m \left\{ \left(\frac{A_{ij}}{r_{ij}^{12}} - \frac{C_{ij}}{r_{ij}^6} \right) (1 - \delta_{ij}^{hb}) + \frac{q_i q_j}{D r_{ij}} + \left(\frac{A_{ij}^{hb}}{r_{ij}^{12}} - \frac{C_{ij}^{hb}}{r_{ij}^{10}} \right) \delta_{ij}^{hb} \right\}, \quad (1)$$

in which

$$A_{ij} = C_{ij} r_{\min}^6 / 2 \quad \text{and} \quad C_{ij} = \frac{3/2 e (\hbar/m^{1/2}) \alpha_i \alpha_j}{(\alpha_i/N_i)^{1/2} + (\alpha_j/N_j)^{1/2}}. \quad (2)$$

In these equations e and m are the electron charge and mass, and q_i and q_j are partial atomic charges for the atoms of the solute and solvent, respectively. D is the dielectric constant ($D=2$), r_{ij} is the distance between atoms i and j of two different molecules in the cluster, α_i is the atomic polarizability of atom i , N_i is the effective number of electrons for each atom type, $r_{\min} = \frac{1}{2}(r_{ii} + r_{jj})$, and r_{ii} and r_{jj} are twice the van der Waals radii of the atoms in the cluster. The α_i and N_i are obtained from Ref. 12, and the q_i are calculated as discussed below. The summation in Eq. (1) is taken so as not to double count any of the atom–atom pairwise interactions for the cluster. δ_{ij}^{hd} is an accounting device which allows hydrogen bonding interactions ($\delta_{ij}^{hb} = 1$) to be modeled (e.g., N, O on the solute radical and N–H and O–H on the solvent molecule, etc.) as appropriate by the potential energy function. For nonhydrogen bonding situations $\delta_{ij}^{hd} = 0$.

The initial approach taken in this work is that Eqs. (1) and (2) should be sufficient to describe the interaction between CNcpd and polar solvents in these small clusters. The terms in the potential should be able to account for electrostatic, induction, depression, and correlation components of the intermolecular interactions at least in a qualitative fashion.¹⁵ The advantage of using this well-known form is that ground state parameters for the atoms are well known and the success rate for the potential is well documented. Calculation for closed shell polar solvent–aromatic clusters are in excellent agreement with the experimental results: closed shell systems such as aniline and benzene–water and ammonia,¹⁶ DMABN/polar solvents¹⁷ and others¹⁸ have been discussed in detail. The task is then to find appropriate parameters for the various terms. For ground state clusters, atomic polarizabilities and atomic vdW radii can be found in the literature.^{12,19,20} The partial atomic charges and geometry of the CNcpd radical and the solvents need to be calculated. For excited state CNcpd, none of these parameters is available and a combination of fitting and calculations must be employed to obtain α_i , r_{ii} , and q_i .

The reason we insist on excited state radical calculations for these studies is that, for the studies we do, only two experimental observables are measured in general: the bare radical $D_1 \leftarrow D_0$ transition²¹ (E_{rad}) and the cluster spectroscopic shift [$\Delta E = (E_{\text{Cl}} - E_{\text{rad}})$]. If an excited state radical calculation is performed (GAUSSIAN 94)¹³ and if both the ground and excited state cluster binding energies can be calculated [Eqs. (1) and (2)], both of these values can be compared with experiments and the complete calculational–analysis algorithm can be verified. van der Waals modes may

TABLE I. Potential parameters for the solvents used in the atom-atom potential calculation. Charges in atomic units, polarizabilities (α_i) in \AA^3 , and vdW radii ($r_{ii}=2r_i$) in \AA .

Molecule	Atom	q_i^a	α_i^b	r_{ii}^c
CF ₂ H ₂	C	0.4886	0.930	4.120
	F	-0.2832	0.557	3.364
	H	0.0389	0.420	2.920
CF ₃ H	C	0.7532	0.930	4.120
	F	-0.2618	0.557	3.364
	H	0.0322	0.420	2.920
CF ₃ Cl	C	0.5430	0.930	4.120
	F	-0.1573	0.557	3.364
	Cl	-0.0711	2.180	3.947
CH ₃ Cl	C	-0.1232	0.930	4.120
	H	0.1056	0.420	2.920
	Cl	-0.1936	2.180	3.947
CH ₃ OH	C	0.2937	1.510	3.740
	H _{CH}	-0.0125	0.420	2.920
	O	-0.6548	0.840	3.120
H ₂ O	H _{OH}	0.3986	0.420	2.830
	O	-0.7460	0.590	3.240
	H	0.3730	0.420	2.830

^aGeometries from Ref. 15. Charges are calculated with the GAUSSIAN 94 program (Ref. 13) at MP2/cc-pVDZ level.

^b α_i of the fluorine is from Ref. 15. The rest are from Ref. 12.

^c r_{ii} of the fluorine is from Ref. 16. The rest are from Ref. 12.

also be identified from some spectra but these features are not always reliably observed in the cluster spectra and often their specific assignments are tentative.

We assume that the presence of the CNcpd (D_1 or D_0) radical does not change any of the solvent properties, and vice versa, and so all calculations are done independently of the other species in the cluster. Atomic charges for solute and solvent species are calculated separately employing the *ab initio* quantum chemistry package GAUSSIAN 94.¹³ Since the structure of all the solvents are known and they remain in their ground electronic and vibrational state during the experiment, a single point second-order Moller-Plesset (MP2/cc-pVDZ basis set) level calculation is employed to obtain their atomic charges. These calculated q_i s are presented in Table I. Both geometry and charges are calculated for CNcpd (see Fig. 1 for the axis system used in this paper) in ground and excited states at the complete active space self-consistent field (CASSCF) (9,9)/cc-pVDZ level. Table II has these results for charges (see also paper I, Tables I and II).

As discussed in paper I of this series, two different methods²² can be used to determine partial atomic charges of the various species of interest: a Mulliken analysis and a potential grid fit to charges to generate calculated molecular electrostatic potential points about the molecule. The Mulliken analysis does not provide accurate values for the q_i because the values depend in an oscillatory way on the calculational method chosen and on the basis set employed; on the other hand, the electrostatic potential grid method does converge and become basis set independent at reasonable levels of theory.

Polarizabilities and vdW radii of the C, N, H atoms comprising CNcpd cannot be calculated readily for the excited electronic state of CNcpd. To find these parameters and carry out binding energy and geometry calculations for excited

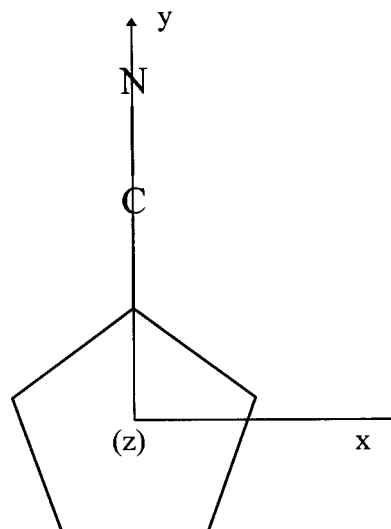


FIG. 1. Schematic diagram and axis system for the CNcpd radical.

state clusters, the various parameters are adopted as given in paper I based on a fit to the CNcpd(Ar)₁ cluster structure and binding energy. The assumptions made in this procedure are discussed in paper I and will be further explored in the Discussion Section below.

III. RESULTS

A. CNcpd(CF₃Cl)₁

The spectrum of the $D_1 \leftarrow D_0$ electronic transition for the CNcpd(CF₃Cl)₁ cluster is presented in Fig. 2. This is the only polar solvent cluster of CNcpd observed in these studies to have a rich vibronic spectrum to the low energy side of the bare radical $D_1 \leftarrow D_0$ absorption 0_0^0 at $27\,144.6\text{ cm}^{-1}$. The cluster transition origin is at $27\,081.6\text{ cm}^{-1}$; the spectral shift for the cluster is -63.0 cm^{-1} . The hole burning spectrum (upper trace of Fig. 2) confirms that all the strong (and some of the weak) features of the fluorescence excitation spectrum for CNcpd(CF₃Cl)₁ arise from the same source, the ground state vibrational level of a single isomer of the cluster. The peak at $27\,065.1\text{ cm}^{-1}$ is 17 cm^{-1} to the red of the cluster origin and it is most likely a hot band.

A striking similarity exists between the spectrum of CNcpd(CF₃Cl)₁ and CNcpd(C₂F₆)₁ (see Fig. 5 of paper I).

TABLE II. Ground and excited states parameters of CNcpd used in the atom-atom potential calculation. Charges in atomic units, polarizabilities (α_i) in \AA^3 , and vdW radii ($r_{ii}=2r_i$) in \AA . Charges are calculated at CASSCF (9,9)/cc-pVDZ level using a potential grid.

Atom	Ground state			Excited state		
	q_i	α_i	r_{ii}	q_i	α_i	r_{ii}
N	-0.5178	0.930	3.510	-0.4520	0.960	3.460
C _{CN}	0.4080	1.150	3.700	0.2429	1.220	3.570
C ₁	-0.2338	1.150	3.700	0.1182	1.294	3.500
C ₂ (C ₅)	0.1149	1.150	3.700	-0.2050	1.294	3.500
C ₃ (C ₄)	-0.1730	1.150	3.700	0.0301	1.294	3.500
H ₂ (H ₅)	0.1043	0.420	2.930	0.1333	0.420	2.930
H ₃ (H ₄)	0.1255	0.420	2.930	0.0871	0.420	2.930

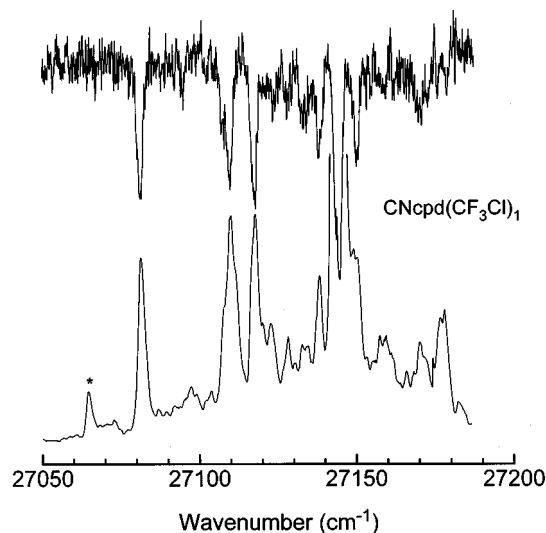


FIG. 2. Fluorescence excitation and hole burning (upper trace) spectra for $\text{CNcpd}(\text{CF}_3\text{Cl})_1$. The vibronic features at 28 and 37 cm^{-1} above the 0_0^0 band are discussed in the text. The feature indicated by an asterisk is a hot band.

The spectral shifts for these two clusters are essentially identical, and the vibrational progressions following the cluster 0_0^0 transitions are also similar: The $\text{CNcpd}(\text{CF}_3\text{Cl})_1$ modes are 28.6 and 36.6 cm^{-1} and those for $\text{CNcpd}(\text{C}_2\text{F}_6)_1$ are 21.7 and 28.8 cm^{-1} . The major difference between the two vibronic patterns is that the z axis stretching mode (σ) for $\text{CNcpd}(\text{CF}_3\text{Cl})_1$ is not as prominent as that for $\text{CNcpd}(\text{C}_2\text{F}_6)_1$.

Atom-atom Lennard-Jones-Coulomb potential energy calculations [Eq. (1)] generate three isomeric structures for the ground state of the cluster, as shown in Fig. 3. The calculated binding energies for these structures are 930, 899, and 779 cm^{-1} for isomers 1-3, respectively. These values are listed in Table III along with those calculated for isomers 1 and 2 for $\text{CNcpd}(\text{C}_2\text{F}_6)_1$ for comparison. Isomer 1 is most likely the most stable one and is probably the isomer observed. In this structure the CF_3Cl molecule lies across the CNcpd ring with the Cl atom beyond the extent of the C_5 -ring. Isomers 1 and 3 have virtually the same structure as those calculated for isomers 1 and 2 of $\text{CNcpd}(\text{C}_2\text{F}_6)_1$, respectively (see paper I, Fig. 6).

The similarity between the observed spectra of $\text{CNcpd}(\text{CF}_3\text{Cl})_1$ and $\text{CNcpd}(\text{C}_2\text{F}_6)_1$ suggests that the Cl atom of CF_3Cl plays a role similar to that of the off-ring CF_3 group of C_2F_6 for cluster intermolecular interactions.

vdW mode calculations²³ for this cluster give six modes for isomer 1 of $\text{CNcpd}(\text{CF}_3\text{Cl})_1$ with energies of 61 (σ), 50 (T_x), 40 (T_y), 30 (b_x), 19 (b_y), and 12 (T_z) cm^{-1} in the D_1 state. A tentative assignment for the 29 and 37 cm^{-1} observed modes would be b_x^1 and b_y^1 with a second member of these progressions also found, through comparison with the observations of paper I. Nevertheless, the excited state potential calculation of the cluster normal modes suggests that they can also be assigned as T_y ($\sim 40 \text{ cm}^{-1}$) and b_x ($\sim 30 \text{ cm}^{-1}$). Under the present circumstances we choose not to make a firm assignment, but we do point out two observations: (1) For this low symmetry system T_y and b_y are not

TABLE III. Binding energies (B.E., in cm^{-1}) estimated for ground and excited state CNcpd clusters by atom-atom potential calculation. Also listed are calculated and experimental spectral shifts of clusters, and dipole moments of solvents.

Solvent	Isomer	B. E.		Shift ^a		Dipole moment (Debye)
		Ground state	Excited state	Calc.	Exp.	
Ar		398	490		-92.0	0.0
CF_4		852	1025	-173	-167.3	0.0
CF_2H_2	1	1032	1056	-24	80.2	1.97
	2	969				
CF_3H	1	1012	1070	-58	87.7	1.65
	2	765	908	-143		
CF_3Cl	1	930	1127	-197	-63.7	0.50
	2	899	1062	-163		
	3	779	934	-165		
C_2F_6	1	900	1068	-168	-62.3	0.0
	2	789	950	-161		
CH_3Cl		972	1208	-236	67.8	1.87
CH_3OH	1	1482	1535	-53	151.0	1.70
	2	1066				
	3	872				
H_2O	1	1245	1264	-19	141.5	1.85
	2	580				
	3	439				

^aThe calculated shift is the difference between the ground and excited state binding energies.

that different; and (2) the anticipated mode intensity would be for b_x and b_y .

B. $\text{CNcpd}(\text{CH}_2\text{F}_2)_x$, $(\text{CHF}_3)_x$, and $(\text{CH}_3\text{Cl})_1$

Spectra obtained for $\text{CNcpd}(\text{CH}_2\text{F}_2)_x$ ($x=1,2$) are shown in Fig. 4. With a low concentration of CH_2F_2 in the expansion gas only one cluster feature appears at 27 224.8 cm^{-1} . This cluster feature is 80.2 cm^{-1} blue shifted from the bare radical 0_0^0 transition, and is assigned as the $\text{CNcpd}(\text{CH}_2\text{F}_2)_1$ cluster 0_0^0 transition. With higher concentrations of CH_2F_2 in the expansion gas another feature appears at 145.9 cm^{-1} from the bare radical origin. This feature is assigned as the $\text{CNcpd}(\text{CH}_2\text{F}_2)_2$ cluster 0_0^0 transition.

As shown in Fig. 5, structure calculations give two isomers for the ground state of $\text{CNcpd}(\text{CH}_2\text{F}_2)_1$ with binding

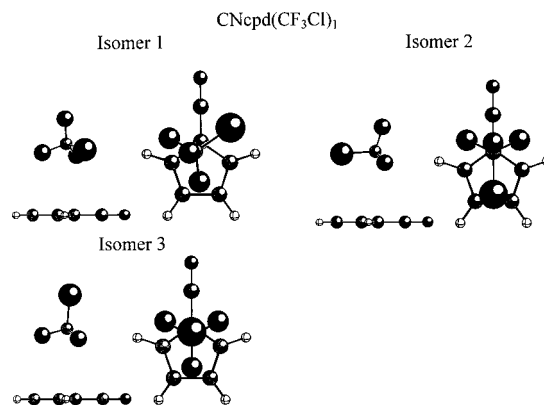


FIG. 3. Calculated ground state isomer structures of the $\text{CNcpd}(\text{CF}_3\text{Cl})_1$ cluster. Isomer 1 is the most stable one.

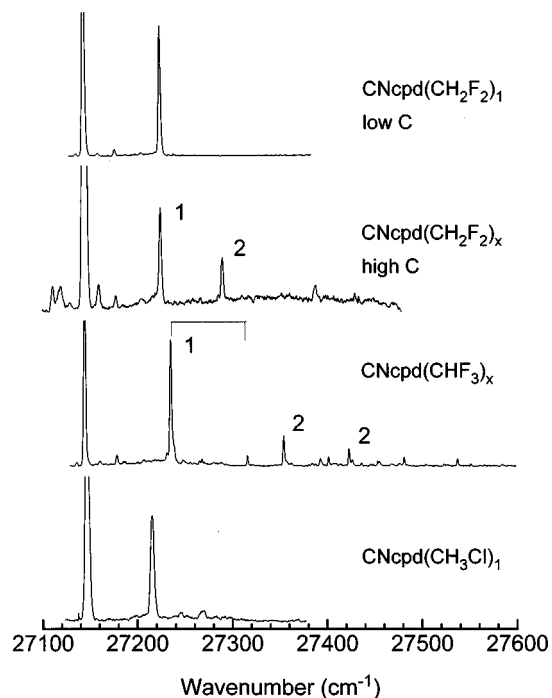


FIG. 4. Fluorescence excitation spectra of CNcpd clustered with various polar solvents as indicated. Numbers on the traces are values of the solvent index x for the particular cluster. High and low C indicate the relative solvent gas concentration in the expansion gas.

energies of 1032 and 969 cm^{-1} . In both instances, the CH_2F_2 solvent molecule is ‘‘off’’ the cpd ring and coordinated to the CN group: The H atoms of CH_2F_2 are closest to the N atom of the CNcpd. The major difference between the two isomer structures is that for isomer 1 both H atoms of the solvent are toward the CN N atom, and for isomer 2, only one of the solvent H atoms is toward the CN N atom. Both

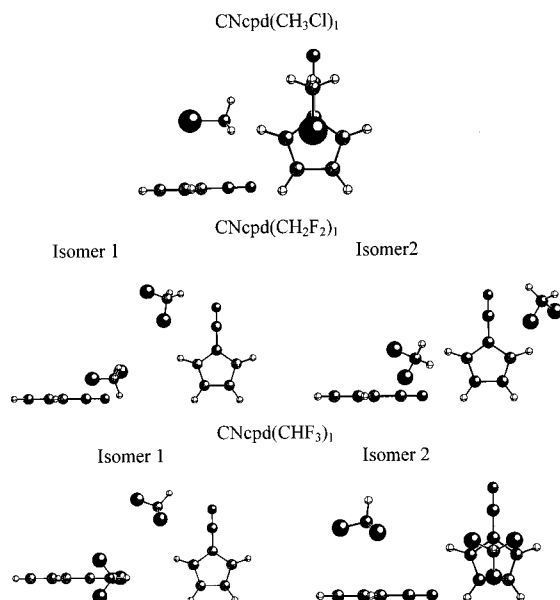


FIG. 5. Calculated ground state isomer structures of $\text{CNcpd}(\text{CH}_3\text{Cl})_1$, $(\text{CH}_2\text{F}_2)_1$, and $(\text{CHF}_3)_1$ clusters. Two isomer structures are calculated for each of the latter two solvents, with Isomer 1 the more stable one in each instance.

structures appear to be generated by a compromise between dipolar, hydrogen bonding, and dispersion interactions. Only one isomer is observed in the spectrum for this cluster, but the barrier to interconversion should be large compared to the final internal temperature of the cooled cluster in the molecular beam, ~ 10 K.

The spectra of $\text{CNcpd}(\text{CHF}_3)_x$, $x=1,2$, clusters are displayed in Fig. 4. Hole burning spectroscopy indicates that the observed cluster related features originate from three sources. The intense feature at $27\,232.5\text{ cm}^{-1}$ and the weak feature at $27\,311.6\text{ cm}^{-1}$ are transitions associated with the same species: They are almost certainly an origin band and a vibronic feature built on it. Two features at $27\,349.5$ and $27\,418.0\text{ cm}^{-1}$ with medium intensity are probably origins for two isomers of the $\text{CNcpd}(\text{CHF}_3)_2$ clusters. These features depend strongly on the concentration of CHF_3 in the backing gas.

Two calculated isomers for the $\text{CNcpd}(\text{CHF}_3)_1$ cluster are found. Isomer 1 in Fig. 5 has the solvent molecule off the cpd ring near the CN groups in a ‘‘dipolar’’ or ‘‘hydrogen bonding’’ like conformation. Isomer 2 has the more traditional van der Waals/dispersion geometry with the three F atoms of CHF_3 coordinated to and on top of the π -ring system. The binding energies for these isomers are 1012 and 765 cm^{-1} , respectively. Isomer 1 is much more stable than isomer 2 and is thus nearly certainly the one observed. The vibrational modes for isomer 1 include the z transitional motion at 75.8 cm^{-1} as the highest energy mode. The observed mode at 79.1 cm^{-1} is probably appropriately assigned as this vibration.

Four different conformations are calculated for ground state $\text{CNcpd}(\text{CHF}_3)_2$ with binding energies of 2028, 1978, 1518, and 1446 cm^{-1} . The most stable of these has the two CHF_3 solvent molecules near the CN moiety in a position similar to that found for isomer 1 of $\text{CNcpd}(\text{CHF}_3)_1$. The second most stable isomer for $\text{CNcpd}(\text{CHF}_3)_2$ is a combination of isomers 1 and 2 for $\text{CNcpd}(\text{CHF}_3)_1$.

The spectrum of $\text{CNcpd}(\text{CH}_3\text{Cl})_1$ possesses only one intense feature as shown in Fig. 4. The cluster spectral shift for this peak is $+67.8\text{ cm}^{-1}$. The cluster structure calculation finds only one stable isomer for this cluster as shown in Fig. 5. The CH_3Cl molecule lies above the CNcpd plane, with the Cl atom nearly over the C_1 ring atom attached to the CN group; the C–Cl bond is nearly parallel to the NC– C_1 bond. The calculated cluster structure has C_s symmetry. Again the structure is ‘‘dipolar’’ and perhaps ‘‘hydrogen bonding’’ in nature, but the Cl atom ring interaction is clearly of a dispersion nature.

C. $\text{CNcpd}(\text{H}_2\text{O})_x$ and $(\text{CH}_3\text{OH})_1$

The spectra of $\text{CNcpd}(\text{H}_2\text{O})_x$ are presented in Fig. 6. These clusters show complicated vibronic structures with a total of 15 features in the $27\,000$ – $27\,600$ region. Hole burning studies are very helpful in identifying features originating from one cluster. The features observed for the $\text{CNcpd}(\text{H}_2\text{O})_x$ clusters can be classified into four groups. The groups can be associated with four transition origins at $27\,233$, $27\,285$, $27\,438$, and $27\,513\text{ cm}^{-1}$, as indicated in Fig.

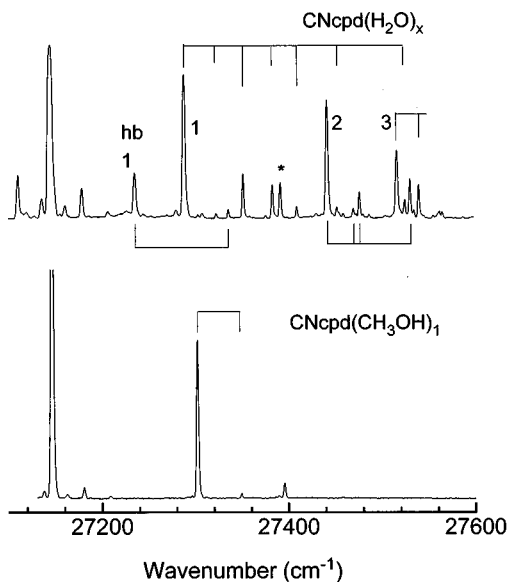


FIG. 6. Fluorescence excitation spectra of CNcpd clustered with H_2O and CH_3OH . Features related to CNcpd with H_2O arise from four sources: Ground state $\text{CNcpd}(\text{H}_2\text{O})_1$, vibrationally hot $\text{CNcpd}(\text{H}_2\text{O})_1$, $\text{CNcpd}(\text{H}_2\text{O})_2$, and $\text{CNcpd}(\text{H}_2\text{O})_3$. Features of the same origin are connected by ticks as determined by hole burning spectroscopy. The peak labeled with an asterisk is assigned to the CNcpd bare radical.

6. One can also vary the concentration of water in the backing gas and note the change in intensity for the four groups of bands. If the water concentration increases in the mixture, the intensity ratio for the 27 233 and 27 285 cm^{-1} features remains the same, while the intensity ratio for the 27 233 and 27 438 cm^{-1} features nearly doubles and that for the 27 233 and 27 513 cm^{-1} features more than doubles. Such intensity ratios allow one to conclude that the two groups of features at energies above 27 400 cm^{-1} belong to $\text{CNcpd}(\text{H}_2\text{O})_x$ ($x > 1$) clusters, while the other two groups belong to $\text{CNcpd}(\text{H}_2\text{O})_1$ clusters.

Calculations generate three structures for $\text{CNcpd}(\text{H}_2\text{O})_1$ but only one of them seems reasonable as a stable structure for the cluster. Figure 7 presents this cluster: the other two have water coordinated to the ring but removed from the π -system and the CN group. These latter potential wells are very shallow, and these structures have binding energies $\frac{1}{2}$ – $\frac{1}{3}$ that of the global minimum (1245 cm^{-1}). This most stable cluster has a hydrogen bonding structure with both H atoms of water attracted to the N atom of the CN group. The distance between the N atom and both H atoms is 2.30 Å. This structure is the only one obtained if small charges are used on the water molecule; we have confidence in the charges calculated for H_2O in this work (see Table I) as they are quite consistent with current values employed by other workers. We thus suggest that the $\text{CNcpd}(\text{H}_2\text{O})_1$ cluster has only one stable structure with a 0_0^0 transition at 27 285 cm^{-1} . The features at 27 233 and 27 332 cm^{-1} probably arise from a vibrationally excited ground state cluster (hot bands), rather than a separate $\text{CNcpd}(\text{H}_2\text{O})_1$ cluster with a different structure.

Structure calculations for $\text{CNcpd}(\text{H}_2\text{O})_2$ give four isomers with binding energies at 4240, 2356, 1850, and 1688 cm^{-1} . The most stable isomer is shown in Fig. 7. In this

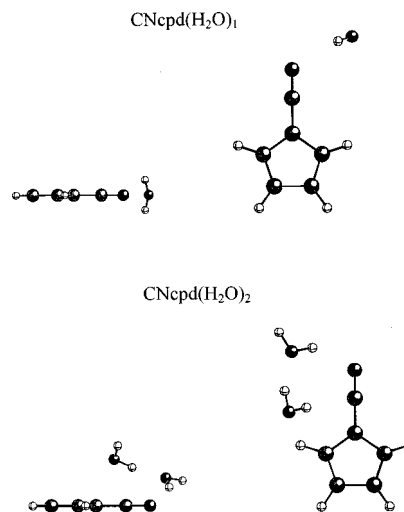


FIG. 7. Calculated most stable ground state isomer structures of CNcpd clustered with H_2O . Four isomer structures are calculated for $\text{CNcpd}(\text{H}_2\text{O})_2$: Only the most stable one is presented in the figure.

structure one water is hydrogen bonded to the N atom of the CN group and the other water molecule is hydrogen bonded to the first. This structure can be thought of a water dimer hydrogen bonded to CNcpd. The lengths of the two hydrogen bonds in this cluster are 2.12 and 1.70 Å for the $\text{N}\cdots\text{H}$ and $\text{O}\cdots\text{H}$ bonds, respectively. The origin band at 27 513 cm^{-1} is assigned as the 0_0^0 transition of this cluster. See the feature labeled 2 in Fig. 6.

Similar calculations identify five isomers for $\text{CNcpd}(\text{H}_2\text{O})_3$ with binding energies at 7190, 4811, 4210, 2959, and 2437 cm^{-1} . Only the most stable one is probably observed and this structure is basically that of a water trimer hydrogen bonded to the N atom of the CN group.

Of all 15 observed water cluster features, seven arise from the ground state level of $\text{CNcpd}(\text{H}_2\text{O})_1$. A three band progression can be identified in this group with a mode of 63 cm^{-1} . The two vibronic bands of this progression are indicated by the long markings and are built on the 0_0^0 transition for $\text{CNcpd}(\text{H}_2\text{O})_1$ clusters indicated by 1 in Fig. 6. The four other vibronic bands built on this origin are 24.1, 94.4, 163.7, and 237.0 cm^{-1} from the origin at 27 285 cm^{-1} . The excited state van der Waals modes for this $\text{CNcpd}(\text{H}_2\text{O})_1$ cluster are calculated at 350.4, 168.0, 159.7, 81.9, 12.2, and 11.9 cm^{-1} . The calculated mode energies are probably not accurate enough for a firm assignment to be made at this time. The feature at 27 233 cm^{-1} labeled hb1 in the figure is probably a hot band associated with the intense 63 cm^{-1} mode of the excited state. Other vibronic features in the spectrum of Fig. 6 are associated with the $\text{CNcpd}(\text{H}_2\text{O})_{2,3}$ cluster origins as indicated.

The spectrum of $\text{CNcpd}(\text{CH}_3\text{OH})_1$ is also displayed in Fig. 6. It consists of only one intense feature and one weak one: The origin is at 27 295.6 cm^{-1} and the weak feature built on it lies at 27 387.9 cm^{-1} . The three calculated isomers for this cluster are given in Fig. 8 and have binding energies of 1482.2 cm^{-1} (1), 1066.4 cm^{-1} (2), and 872.2 cm^{-1} (3). The observed isomer is identified as isomer 1 due to the large binding energy and strong $-\text{CN}\cdots\text{H}-\text{OCH}_3$ hydrogen bond-

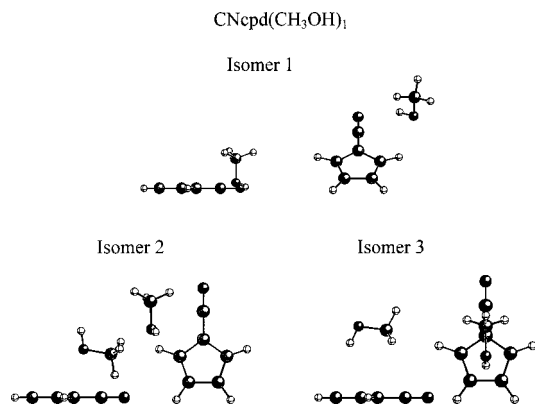


FIG. 8. Calculated ground state isomeric structures of CNcpd clustered with CH₃OH. Isomer 1 is the most stable one.

ing structure. The N··H distance is 2.27 Å for this structure. The spectral blue shift for this cluster is $\sim 150\text{ cm}^{-1}$, very close to that observed for CNcpd(H₂O)₁. The 88 cm⁻¹ vibronic feature built on the 0₀⁰ transition is not assigned to a specific mode.

IV. DISCUSSION

A. Polar and nonpolar solvents—cluster shifts and structures

With the exception of CF₃Cl, which behaves very much like CF₃CF₃, all nonpolar solvents have red shifted $D_1 \leftarrow D_0 0_0^0$ transitions and all polar solvents have blue shifted $D_1 \leftarrow D_0 0_0^0$ transitions for the clusters with respect to the bare CNcpd radical transition. One usually thinks of cluster transition shifts as due to the difference in cluster binding energies for the ground and excited state cluster: a red shift implies that the excited state is more tightly bound than the ground state and a blue shift implies that the ground state is more tightly bound than the excited state. Typical dispersion interactions, such as modeled well by the Lennard-Jones form, give rise to red shifted cluster spectra. These interactions depend on polarizabilities and typically the ground state of the solute is less polarizable than the excited state (the excited electron is less tightly bound to the core) and the excited state vdW potential well is thus deeper than the ground state one. For polar molecules, atomic partial charges (and their spatial arrangements as described by molecular multipolar moments) begin to become important for the intermolecular interactions in a cluster. Since Eq. (1) has a Coulomb term, and since this term is expressed in atomic partial charges and their geometrical distribution, Eq. (1) should be able to account for molecular dipole–dipole, quadrupole–quadrupole, dipole–quadrupole, etc. interactions, at least partially. Equation (1) also accounts for hydrogen bonding interactions for special cases like N··H–N–, N··H–O–, O··H–O–, etc. Equation (1) probably does not account well for induced interactions, which can in principle become important for highly polar systems.^{15,24} For large induced interactions, the calculated and fit potential parameters based on vdW interactions and isolated molecular prop-

erties (e.g., partial atomic charges q_i and structures) would no longer be a reasonable approximation for the cluster potential function.²⁵

Solvent polarity also seems to have a controlling effect on cluster structure. Nonpolar solvents interact with aromatic systems (molecules or radicals) through the aromatic π -system and the solvent region of high electron density, as is expected for dispersion interactions. Polar solvents, on the other hand, assume a cluster geometry that is clearly not of this form and may even be characterized as “dipolar” or “hydrogen bonding.” Note, however, the systematics of cluster shift and solvent dipole moment as expressed in Table III; at least cluster shifts are not “dipolar” or “charge transfer” in nature. Additionally, the two largest blue shifts are for the hydrogen bonded system (H₂O and CH₃OH). All the calculated shifts are red shifts, perhaps because the CNcpd $\mu(D_0) = 5.14\text{ D}$ and $\mu(D_1) = 6.29\text{ D}$, while the experimental ones are generally blue shifts for polar solvents. The exception to this rule is CF₃Cl, which assumes the standard nonpolar solvent geometry above the ring π -system for the CNcpd(CF₃Cl)₁ cluster. This result, that the one experimental red shift is associated with the one calculated dispersion cluster geometry, is actually a nice validation of the employed potential energy surface and algorithm.

B. Cluster potential energy surface calculations

Consider first the nature of the disagreement we must address. The differences between calculated and experimental values for the cluster shifts are systematic; that is, the calculated shifts for CNcpd(polar solvent)₁ clusters are all red (-20 to -240 cm^{-1}) and those observed are all blue ($+68$ to $+150\text{ cm}^{-1}$, except for CF₃Cl), as displayed in Table III. The shifts do not scale with dipole moment of the solvent (Table III); nor are they related to the increase in dipole moment for the D_1 to D_0 transition, as this would generate a red shift. The shifts do not scale with hydrogen bonding as one can see from the charges on H in CF₃H and CH₃Cl shown in Table I, although the largest shifts are for H₂O and CH₃OH. The small charges on the H atoms of CH_{4-n}X_n should suggest that in these case hydrogen bonding is not likely. In fact, the hydrogen bonding term in Eq. (1) is only activated for CH₃OH and H₂O solvents; nevertheless, the polar cluster structures are certainly reminiscent of expected hydrogen bonding like structures. Additionally, and not surprisingly, the shifts do not scale with solvent polarizability or solvent ionization energy; this, of course, rules out charge transfer contributions as a controlling factor for the observed shifts.

The cluster spectral shift is certainly a very stringent test of the entire set of calculations: it basically requires that the ground and excited state calculated binding energies are good to better than $\pm 10\%$. The fact that these differences between calculated and experimental shifts are systematic gives one reason to look for a general cause for lack of agreement.

The major source of error probably arises from atomic parameters α_i , r_i used in estimating dispersion interactions. First, for polar solvent clusters, the electric field generated by the solvent can change or polarize the CNcpd so that the

dispersion parameters α_i and r_i determined for the different atoms of CNcpd for nonpolar environment, are no longer appropriate. Recall that the ground state α_i and r_i values come from crystallographic results typically and the excited state α_i and r_i are approximated from Xcpd(Ar)₁ shifts. Second, the potential parameter calculational process is simplified for the excited state Xcpd radical by assuming that the interactions between solvent and the radical are mainly solvent–ring carbon interactions, while the interactions between solvent and the hydrogen atoms for Xcpd are the same in ground and excited state clusters. While this approximation seems reasonable and is valid for nonpolar solvent clusters, it may be a significant source of error in estimating the excited state binding energy of Cncpd(polar solvent)₁. The polar solvent molecule may strongly interact with the ring hydrogen atom(s) close to it. Cluster structure for Xcpd–polar and nonpolar solvent clusters can be very different. Third, contribution to the calculated binding energy error in both ground and excited state clusters can arise from the inadequacy of the polar solvent α_i and r_i atomic parameters. For example, the C and H parameters used for CH₂F₂ come from parameters derived for CH₄. For polar molecules such approximate parameters are worse than for nonpolar systems: such an error may be even worse for excited states. Fourth, if the potential energy surface function of Eq. (1) is employed using excited state charges and structures but ground state α_i and r_i values, the calculated cluster spectral shifts are either small red or blue shifts. This observation suggests that the potential form employed is reasonable, but that one of the major problems for the calculated shifts is the excited state atomic parameters α_i and r_i used for CNcpd. These parameters are obtained through fitting the spectroscopic shift of CNcpd(Ar)₁, a dispersion interaction dominated cluster. Note that the structure of these polar solvent clusters is different from that of the nonpolar solvent clusters.

Calculation errors are also expected to arise through the Coulomb terms: Xcpd(Ar)₁ has no Coulombic interaction. Therefore, Coulombic interaction is not subject to fitting and must rest on atomic charges calculated for isolated molecules. While this approximation is not of concern for nonpolar solvent clusters, for which the Coulomb interaction is small, contributions from this type of interaction become significant for clusters discussed in this study, especially for large induced interactions. Thus 10%–20% errors in this term now leave the calculated shift systematically in error. The isolated molecule and radical atomic charge calculations are probably quite accurate based on the results of paper I in this series and the fact that the CNcpd $D_1 \leftarrow D_0$ transition energy is calculated to $\pm 500 \text{ cm}^{-1}$.

The spectroscopic shift direction is a balance between Coulomb and dispersion terms in the potential. Apparently strong Coulomb interactions give rise to positive shifts and large dispersion interactions give rise to negative shifts.

The calculated cluster structures are probably accurate or at least appropriate because a wide range of q_i 's, α_i 's, and r_i 's give roughly the same cluster structures with only $\pm 10\%$ to $\pm 20\%$ variations in cluster binding energies. Within this variation the cluster spectral shifts can be accommodated,

but considering their general systematic behavior, a more fundamental investigation of the disagreement between calculated and experimental shifts is appropriate as discussed above. Calculated ground and excited state structures are very similar in all respects and the cluster spectra are consistent with this similarity.

vdW modes are calculated for all the clusters and are not well represented for excited state clusters in the harmonic approximation. Since the cluster spectroscopic shift is systematically incorrect for these clusters, the balance between Coulomb and dispersion interactions is incorrect due to inaccurate potential parameters, and thus the potential shape in the excited state may be misrepresented. Under these circumstances, the vdW modes of the clusters in the harmonic approximation cannot be expected to be accurate.

V. CONCLUSIONS

We have studied the solvation of CNcpd by several polar solvent molecules employing fluorescence excitation and hole burning spectroscopy, *ab initio* calculations for CNcpd charges and structures, and cluster potential energy surface calculation with a Lennard-Jones–Coulomb form. Almost all of these clusters show blue shifted spectra and a structure reminiscent of a dipolar or a hydrogen bonding geometry. The shifts do not scale well with dipole moment of the solvent molecule, but the largest blue shifts are for H₂O and CH₃OH, the only hydrogen bonding solvents in the group chosen. Cluster structures and binding energy seem reasonable based on these calculations, but the cluster spectral shifts are systematically incorrect suggesting that the cluster Lennard-Jones van der Waals parameters (α_i and r_i) are not well determined for the excited electronic state and/or that the calculated charges for the isolated species are inappropriate for the clusters. The Lennard-Jones–Coulomb potential form seems to be adequate to account for the general structures and binding energies of this open shell radical–polar solvent set of clusters. Cluster properties appear to be a balance between coulomb and dispersion–induction terms in the potential. Calculated harmonic vdW modes are not typically accurate enough for the excited electronic state of the clusters for reliable mode assignment, probably due to both the harmonic approximation and the potential parameters.

The next advance in treating the energetics and vibrational mode structure for these clusters and other polar solvent clusters would be to obtain better potential parameter values for the excited state cluster surface.

ACKNOWLEDGMENTS

These studies were supported in part by grants from USARO and USNSF. J.A.F. wishes to thank the Basque government for a postdoctoral fellowship.

¹ See for example M. C. Heaven, *Annu. Rev. Phys. Chem.* **43**, 283 (1992); E. R. Bernstein, *ibid.* **46**, 197 (1995); Q. Y. Shang and E. R. Bernstein, *Chem. Rev.* **94**, 2015 (1994); M. I. Lester, *Adv. Chem. Phys.* **96**, 51 (1996); *Chemical Reactions in Clusters*, edited by E. R. Bernstein (Oxford University Press, N. Y., 1996); P. Hobza, H. L. Selzle, and E. W. Schlag, *Chem. Rev.* **94**, 1767 (1994); P. Hobza and R. Zahradnik, *ibid.* **88**, 871 (1988); A. D. Buckingham, P. W. Fowler, and J. M. Hutson, *ibid.* **88**, 963

- (1988); E. R. Bernstein, in *Atomic and Molecular Clusters*, edited by E. R. Bernstein (Elsevier, New York, 1990), p. 551.
- ²D. Fulle, H. F. Hamann, H. Hippler, and J. Troe, *J. Chem. Phys.* **105**, 983 (1996); R. A. Loomis, R. L. Schwartz, and M. I. Lester, *ibid.* **104**, 6984 (1996); W. M. Fawzy and M. C. Heaven, *ibid.* **92**, 909 (1990); J. L. Lemaire, W.-Ü. L. Tchang-Brillet, N. Shafizadeh, F. Rostas, and J. Rostas, *ibid.* **91**, 6657 (1989).
- ³R. W. Randall, C. Chuang, and M. I. Lester, *Chem. Phys. Lett.* **113**, 200 (1992).
- ⁴M. J. McQuaid, G. W. Lemire, and R. C. Sausa, *Chem. Phys. Lett.* **210**, 350 (1993); G. W. Lemire, M. J. McQuaid, and R. C. Sausa, *J. Chem. Phys.* **99**, 91 (1993).
- ⁵W. G. Lawrence, Y. Chen, and M. C. Heaven, *J. Chem. Phys.* **107**, 7163 (1997); M. Yang and M. H. Alexander, *ibid.* **107**, 7148 (1997), and references therein.
- ⁶S. A. Wright and P. J. Dagdigian, *J. Chem. Phys.* **107**, 680 (1997).
- ⁷L. J. van de Burgt and M. C. Heaven, *J. Chem. Phys.* **89**, 2768 (1988).
- ⁸J. A. Fernández, J. Yao, and E. R. Bernstein, *J. Chem. Phys.* **107**, 3363 (1997).
- ⁹J. Yao, J. A. Fernández, and E. R. Bernstein, *J. Chem. Phys.* **107**, 8813 (1997).
- ¹⁰R. Disselkamp and E. R. Bernstein, *J. Chem. Phys.* **98**, 4339 (1993); *J. Phys. Chem.* **98**, 7260 (1994).
- ¹¹S. Sun and E. R. Bernstein, *J. Chem. Phys.* **103**, 4447 (1995); L. Yu, J. Williamson, S. C. Foster, and T. A. Miller, *ibid.* **97**, 5273 (1992).
- ¹²R. A. Scott, and H. A. Scheraga, *J. Chem. Phys.* **45**, 2091 (1966); F. A. Momany, L. M. Carruthers, R. F. McGuire, and H. A. Scheraga, *J. Phys. Chem.* **78**, 1595 (1974); F. A. Momany, R. F. McGuire, A. W. Burgess, and H. A. Scheraga, *ibid.* **79**, 2361 (1975); G. Némethy, M. S. Pottle, and H. A. Scheraga, *ibid.* **87**, 1883 (1988); R. A. Scott and H. A. Scheraga, *J. Chem. Phys.* **42**, 2209 (1965).
- ¹³GAUSSIAN 94, M. J. Frisch, G. W. Trucks, H. B. Schlegel, P. M. W. Gill, B. G. Johnson, M. A. Robb, J. R. Cheeseman, T. A. Keith, G. A. Petersson, J. A. Montgomery, K. Raghavachari, M. A. Al-Laham, V. G. Zakrzewski, J. V. Ortiz, J. B. Foresman, J. Cioslowski, B. B. Stefanov, A. Nanayakkara, M. Challacombe, C. Y. Peng, P. Y. Ayala, W. Chen, M. W. Wong, J. L. Andrés, E. S. Replogle, R. Gomperts, R. L. Martin, D. J. Fox, J. S. Binkley, D. J. Defrees, J. Baker, J. P. Stewart, M. Head-Gordon, C. González, and J. A. Pople, Gaussian Inc., Pittsburgh, PA, 1995.
- ¹⁴R. O. Lindsay and C. F. H. Allen, *Organic Syntheses Collective*, edited by E. C. Horning (Wiley, London, 1955), Vol. 3, pp. 710–711.
- ¹⁵A. J. Stone, *The Theory of Intermolecular Forces* (Oxford University Press, Oxford, 1996).
- ¹⁶J. A. Menapace and E. R. Bernstein, *J. Phys. Chem.* **91**, 2533 (1987); J. A. Fernandez and E. R. Bernstein, *J. Chem. Phys.* **106**, 3029 (1997).
- ¹⁷V. H. Grassian, J. A. Warren, and E. R. Bernstein, *J. Chem. Phys.* **90**, 3994 (1989); J. A. Warren, E. R. Bernstein, and J. I. Seeman, *ibid.* **88**, 871 (1988).
- ¹⁸S. K. Kim and E. R. Bernstein, *J. Phys. Chem.* **94**, 3531 (1990); M. R. Nimlos, D. F. Kelley, and E. R. Bernstein, *ibid.* **93**, 643 (1989); S. K. Kim, S. Li, and E. R. Bernstein, *J. Chem. Phys.* **95**, 3119 (1991); S. K. Kim, S. C. Hsu, S. Li, and E. R. Bernstein, *ibid.* **95**, 3290 (1991); S. Li and E. R. Bernstein, *ibid.* **97**, 792 (1992); S. Li and E. R. Bernstein, *ibid.* **97**, 804 (1992); Q. Y. Shang, P. O. Moreno, and E. R. Bernstein, *J. Am. Chem. Soc.* **116**, 302 (1994); Q. Y. Shang and E. R. Bernstein, *Chem. Rev.* **94**, 2015 (1994).
- ¹⁹*Handbook of Chemistry and Physics*, 76th ed. (CRC, Boca Raton, Florida, 1995).
- ²⁰A. K. Rappe, C. J. Casewit, K. S. Colwell, W. A. Goddard III, and W. M. Skiff, *J. Am. Chem. Soc.* **114**, 10026 (1992).
- ²¹See Ref. 29 of paper I.
- ²²C. M. Breneman and K. B. Wiberg, *J. Comput. Chem.* **11**, 361 (1990).
- ²³S. Li and E. R. Bernstein, *J. Chem. Phys.* **95**, 1577 (1991); J. A. Menapace and E. R. Bernstein, *J. Phys. Chem.* **91**, 2533 (1987); E. B. Wilson, J. C. Decius, and P. C. Cross, *Molecular Vibrations* (Dover, New York, 1980).
- ²⁴J. O. Hirschfelder, C. F. Curtiss, and R. B. Bird, *Molecular Theory of Gases and Liquids* (Wiley, New York, 1964).
- ²⁵L. X. Dang, J. E. Rice, J. Caldwell, and P. A. Kollman, *J. Am. Chem. Soc.* **113**, 2481 (1991); J. Caldwell, L. X. Dang, and P. A. Kollman, *ibid.* **112**, 9144 (1990); I. Benjamin, D. Evans, and A. Nitzan, *J. Chem. Phys.* **106**, 6647 (1997).